Computational Optimization of a Rotary Valved Pulse Combustor Concept

Daniel E. Paxson[1] and H. Douglas Perkins[2]
NASA Glenn Research Center, Cleveland, Ohio, 44135

Shaye Yungster[3]
HX5, LLC, NASA Glenn Research Center, Cleveland, Ohio, 44142

A resonant pulse combustor valve concept is introduced that utilizes two slotted, coaxial counterrotating discs for mechanical actuation at the combustor inlet. The intended test article for prototype demonstration is a small, 22 in. long, propane fueled laboratory combustor, flowing approximately 0.006 lbm/s of air. The objective is to develop an externally actuated (i.e., active) valve that yields better performance and longer life than the traditional internally actuated (i.e., passive), reed-type valve found on most pulse combustors. The rotary valve motion is optimized using an axisymmetric, two-dimensional computational fluid dynamic simulation with a domain that includes the valve as a moveable interior wall. Parameters such as slew rate, dwell period in the open position, and total closed period are varied using fuel specific impulse as the figure of merit. Variations in fuel injector location and air fuel ratio are also examined. Additionally, the performance impact of leakage from the rotary valve is quantified since leakage is endemic to the design. The optimized simulation results indicate that the rotary valve concept can deliver the desired performance attributes using disc rotational speeds and stresses that are well within the realm of modern materials. A preliminary mechanical valve design is included in the report.

Nomenclature

A	=	valve area
A_{open}	=	inlet cross sectional area when the valve is fully open
ER	=	equivalence ratio
I_{sp}	=	fuel specific impulse
T	=	temperature
T_0	=	ambient temperature
τ_{oc}	=	opening and closing periods (valve is partially open or closed)
τ_{dwell}	=	period when valve is fully open
τ_{closed}	=	period when valve is fully closed

I. Introduction

Resonant Pulse Combustors (RPC) represent the highest performing implementation approach to Pressure Gain Combustion (PGC) reported to date. PGC, by definition, yields a total pressure rise across the device in which it is implemented. While Rotating Detonation Combustors (RDC's) have to date demonstrated pressure gains at or below 0.2% [1, 2], Internal Combustion Wave Rotors (ICWR's) have demonstrated gains of 5%-17% [3], and Pulse Detonation Engines (PDE's) have demonstrated unspecified but publicly stated positive gains [4], RPC's have demonstrated pressure gain in excess of 50% [5] as measured using the Equivalent Available Pressure (EAP) approach

[1] Aerospace Research Engineer, Research and Engineering Directorate, AIAA Associate Fellow
[2] Aerospace Research Engineer, Research and Engineering Directorate, AIAA Senior Member
[3] Aerospace Research Engineer, Research and Engineering Directorate, AIAA Senior Member

outlined in [6]. These pressure gain values reflect devices operating with fuel/air ratios ranging from near stoichiometric to somewhat rich. When they are combined with ejector technology to reduce the overall air/fuel ratios (i.e., exhaust temperatures) to gas turbine compatible values, Ejector Enhanced RPC's (EERPC) can still generate approximately 4% pressure gain [7, 8]. Furthermore, detailed computational fluid dynamic (CFD) simulations have indicated that the EERPC configuration can work well at the high pressures and temperatures associated with modern gas turbines, while simultaneously producing competitively low emissions [9]. The thermodynamic benefits of EERPC pressure gain are substantial in terms of reduced specific fuel consumption (and associated greenhouse gas reduction) [8]. The demonstrated capability to operate with liquid or gaseous fuels also makes RPC attractive for use in the gas turbine environment.

High performance RPC's do have significant challenges however, and chief among these is the requirement of a mechanical air inlet valve. Following [10] and with reference to Fig. 1, the periodic RPC cycle may be described as having four stages. First, air enters the combustion chamber through the open inlet valve. It is mixed with fuel as it enters. Second, the mixture is ignited and undergoes a rapid, confined combustion process. Confinement is provided on the inlet end by the inlet valve, which closes as the pressure rises in the chamber. Confinement at the outlet is provided by the fluid in the tailpipe and its associated inertia. Third, combustion produces a rapid rise in the chamber pressure. This propagates a compression wave down the tailpipe and accelerates the fluid therein. The accelerated fluid rapidly exits the tailpipe allowing expansion of the combustion chamber products. Fourth, due to the combined expansion process (aka, blowdown) and reflection of gasdynamic waves from the open end of the tailpipe, the chamber pressure eventually drops below the ambient pressure. The inlet valve then opens and allows a new charge of air and fuel to enter. The low chamber pressure also decelerates the exiting tailpipe fluid to such a degree that it briefly reverses direction. The reversed hot combustion products ignite the fresh charge, and the cycle begins anew. A more detailed illustration of the cycle may be found in [9]. Therein it is shown that there exists a complex combination of acoustic, Helmholtz, mixing, chemical kinetic, coherent vortex, evaporative, and mechanical time scales that must couple constructively to achieve successful resonant operation. The overall operational frequency of this process depends on many factors, but it is dominated by the combined combustion chamber and tailpipe length. For pulse combustors that are appropriate for gas turbine applications, this implies operation at several hundred hertz. The chamber pressure during operation typically oscillates from approximately twice to one half of the ambient (or compressor discharge) pressure. Designing an air valve that can simultaneously operate at these frequencies, sustain the harsh combustor pressure and temperature environment, and fit within the geometric constraints of the combustor is a significant technological challenge. Adding to this challenge is the observation that the particular motion of the valve required for high performance operation is complex [11-13].

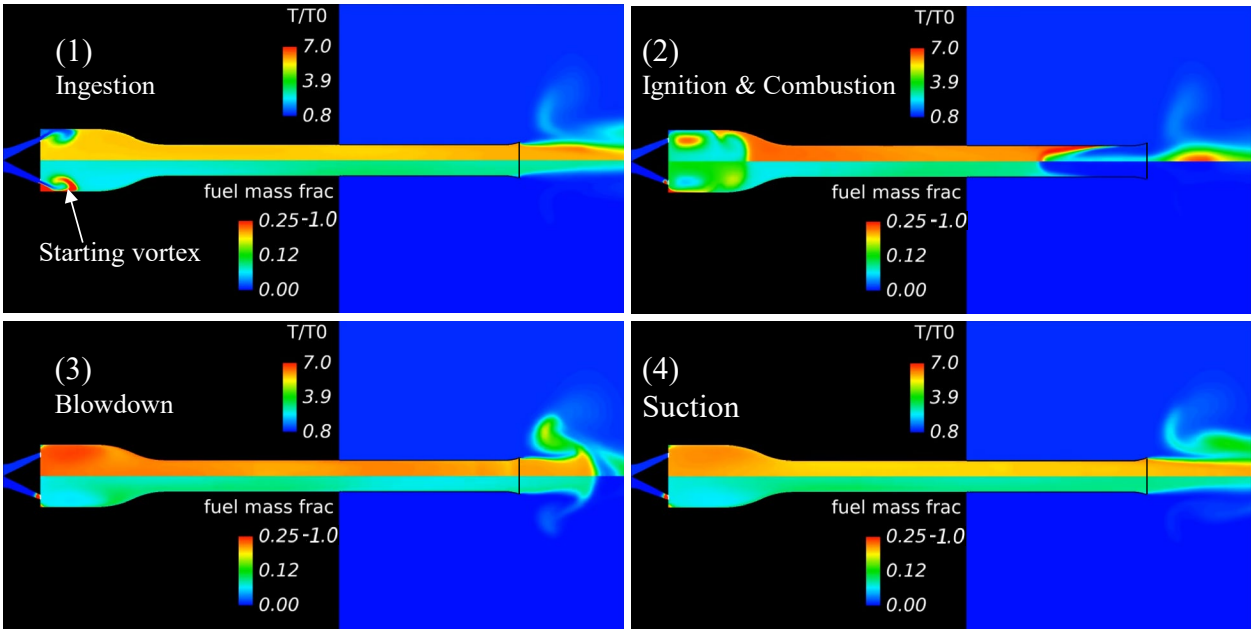

Fig. 1 Computational Fluid Dynamic simulated contours of temperature (upper half) and fuel mass fraction (lower half) from [13] illustrating the four stages of the RPC process in a reed-valved combustor

Many high frequency pulse combustors utilize a passive (i.e., actuated by internal fluid and mechanical forces), reed-type inlet valve [13]. The design was originated by the Curtis Dyna-Fog Company in approximately 1950. Although the valve delivers the requisite motion, it does not last long. The harsh thermal environment, significant flexure on opening, and subsequent rapid deceleration (i.e., slamming) on closing can result in valve failure after only minutes of cumulative run time. A variation of the reed valve design using high temperature poppet valves and external springs was fabricated and tested at NASA's Glenn Research Center in 2023 [13]. However, it did not achieve resonant operation. The conclusion drawn from the effort was that passive valves cannot simultaneously provide the requisite motion and last for extended periods.

Robust, active valves (i.e., externally actuated) with exceptionally long lifetimes have been fabricated and tested [14]. Unfortunately, the resulting combustor performance has been below that of the original reed-valved units in terms of pressure gain. The reason for this is likely that their motion (e.g., duty cycle, slew rate, phase angle, etc.) is not quite matched to the other time scales. Furthermore, the active designs to date do not generally have independently variable parameters. And finally, recent active valve designs do not generate a single coherent starting vortex during the inflow period, which has been recognized as a critical feature for high performance [9]. This vortex is just visible on the left side of the first contour of Fig. 1.

The present work considers a novel active inlet valve design that utilizes two slotted counterrotating discs with minimal clearance between them. The discs are arranged with their faces perpendicular to the combustor axis of rotation (the dominant flow direction) such that they penetrate the inlet channel of the combustor. Through rotation, the discs and their associated slots act like a double-edged knife-valve. The valve concept will be detailed in the first section of the paper. Following this, the motion will be optimized by embedding the valve in a validated, axisymmetric, two-dimensional (2D) computational fluid dynamic (CFD) simulation of an existing laboratory scale pulse combustor which is planned as a future test article for the concept [13]. Optimization will be performed by first choosing a nominal opening and closing rate for the valve based on an expected operating frequency of 200 Hz., an estimated disc diameter of 4.76 in., and a disc rotational speed of 6000 rpm. From here the dwell time (i.e., the amount of time that the valve is fully open), and the fully closed time will be parametrically varied. For each dwell and closed time examined, the simulation is run until a limit cycle is achieved. The figure of merit for each dwell and closed time tested is fuel specific thrust (aka, specific impulse). Other parameters will be examined in this same manner including the radial position of the fuel injectors, and the air/fuel ratio. Finally, the impact of valve leakage on performance will be examined since this valve concept will, as explained below, allow some leakage. The simulation results demonstrate that if the valve can be designed to produce the optimized motion, the pulse combustor performance will exceed that of the existing reed-valved unit.

A preliminary mechanical design of the optimized valve will then be presented, indicating that its fabrication is well within the realm of conventional practices.

II. Rotary Valve Concept

A top view of the proposed valve is shown schematically in Fig. 2. The figure is approximately to scale, and the dimensions (inches) are such that it would mate to the existing laboratory combustion chamber and tailpipe [13]. The flow diverter presented has not yet been optimized. It represents a nominal geometry that will be used throughout the present study. It would be held in place by struts, which are not shown. The propane fuel would be introduced through a series of holes that are approximately located in the position shown by the green arrows (though they could also be located on the diverter struts, or on the diverter itself. Leakage can occur at the indicated location, although the gap is expected to be much smaller than what is shown. Leakage will reduce the amplitude of the pressure pulse developed during each confined combustion event, which ultimately lowers performance.

A front view of the same valve is shown in Fig. 3. Each disc has 2 slots placed 180 degrees apart. Thus, there are two cycles executed per complete disc rotation. The initial slots shown, at the initial 6000 rpm speed, produce opening and closing periods, τ_{oc}, of 0.5 msec., a dwell period, τ_{dwell}, of 1.0 msec. and a fully closed period, τ_{closed}, of 3.0 msec. The design concept leaves flexibility in each of these parameters depending on the disc diameter, slot geometry, number of cycles per revolution, and rotational speed. Figure 3 also shows the opening process (top row) and closing process (bottom row) as a series of three snapshots of the disc position. The discs are color coded and drawn semi-transparent so that all slot positions can be seen. Note that the opening and closing processes are nearly symmetric about the centerline. This ensures the production of the important coherent starting inlet vortex pointed out in Fig. 1 (first panel). If only one disc were used, the opening period would be longer, and it would proceed from one side to the other of the inlet.

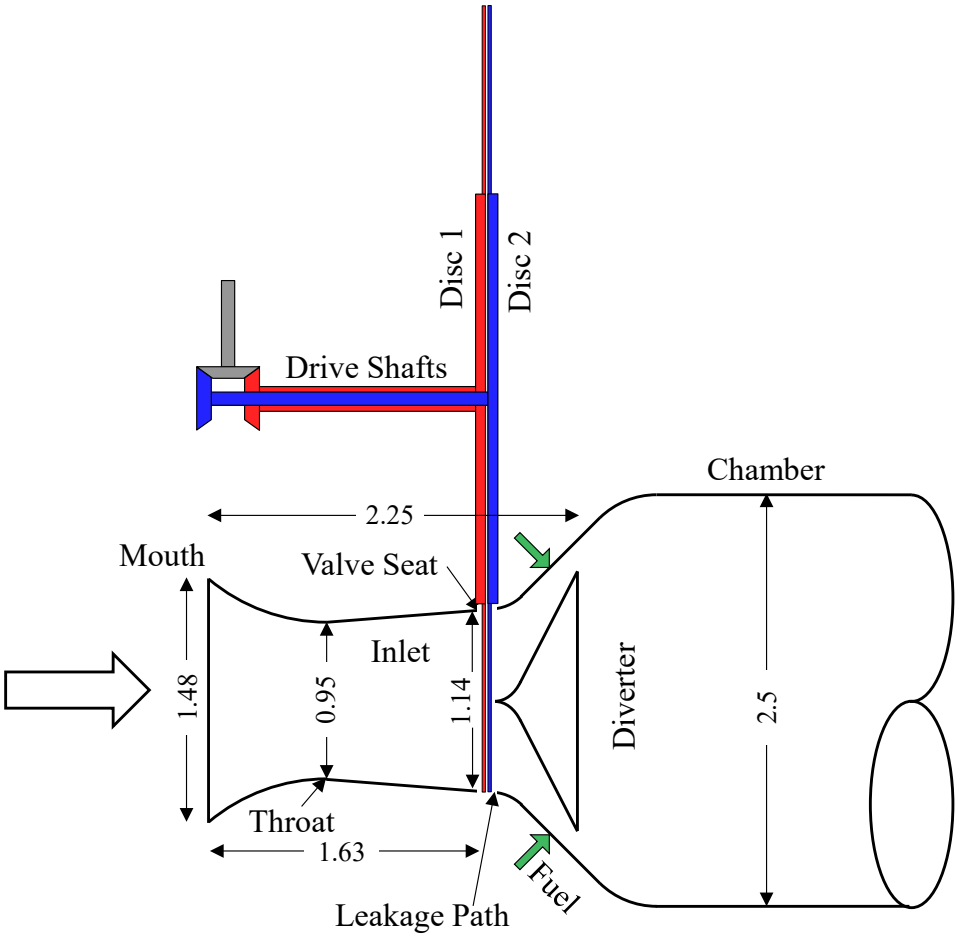

Fig. 2 Schematic top view of rotary disc pulse combustor valve (dimensions are inches)

The area versus time can easily be calculated for the valve. For this initial design it is shown in Fig. 4. Here, A_{open} is the inlet cross sectional area when the valve is fully open.

III. CFD Optimization

The CFD simulation used for this work has been detailed and validated previously [9, 13, 15]. As such only a brief description is provided here. It is an in-house code which solves the axisymmetric, unsteady, Reynolds averaged Navier-Stokes (URANS) equations for a multi-species, thermally perfect, chemically reacting gas. The turbulence model used in the calculations is the Spalart-Allmaras one-equation model. The fuel is propane with a kinetics mechanism based on the 10-species, 10-reaction ethylene mechanism of Ref. [16] where ethylene is replaced with propane. Additional detail is found in Appendix A1. The computational domain includes the interior of the pulse combustor, some free space downstream of the tailpipe exit plane so that the well-known vortex that is emitted each pulse can be captured, and a zone of free space near the leakage region of the valve. The combustor walls are assumed adiabatic with no-slip. The outer surfaces of the free spaces use a constant ambient pressure boundary condition. The pulse combustor inlet plane is maintained at constant total pressure and total temperature, with the values being equal to the ambient pressure and temperature. Solutions are obtained on the NASA Advanced Supercomputer (NAS). Typical simulations have approximately 160,000 grid points and require approximately 16 wall hours per cycle (using 22 processors), with 8-12 cycles required to achieve limit cycle operation. Figure 5a shows the entire computational space using a reduced grid cell count for improved visualization. The retractable wall used to simulate the valve is shown in Fig., 5b. The wall approximates the continuous valve motion through a series of discrete jumps of the tip from one radial grid point to the adjacent grid point at the time dictated by the prescribed motion of Fig. 4. The 0.01 in. maximum leakage gap is shown in Fig. 5c. It is noted that the computational leakage gap has a different orientation

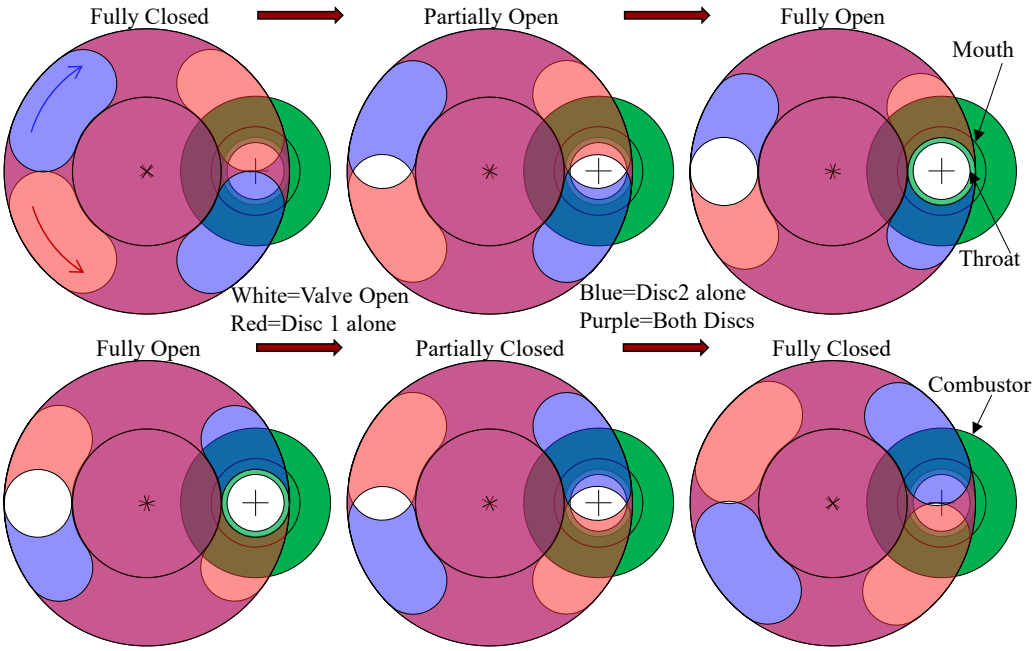

Fig. 3 Schematic front view of rotary disc pulse combustor valve showing opening (top row) and closing (bottom row) processes as the discs counterrotate

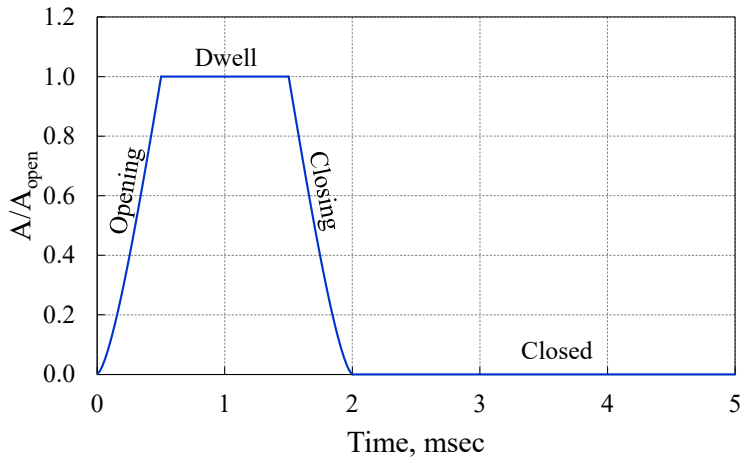

Fig. 4 Valve opening for the initial rotary valve geometry as a function of time

than that of Fig. 2. This orientation was simpler to include in the grid and achieved the same effect as the actual leakage gap.

Fuel injection occurs through the continuous wedge shaped ring shown in Fig. 5c. This approximates the discrete injection holes envisioned for the laboratory experiment. Fuel flow is pressure driven. The wedge is fed by a notional manifold held at a total pressure prescribed by the user. When the static pressure on the downstream face of the wedge is below the manifold pressure, fuel flows according to standard compressible, isentropic relationships, and proportionally to the wedge cross sectional area. If the static pressure is above the manifold pressure, a 'check-valve' is activated which stops backflow of fuel into the manifold. Finding the manifold pressure necessary for a specified mixture ratio is an iterative process. A pressure is guessed, the simulation is run to a limit cycle solution, the average mixture ratio is checked, and manifold pressure is adjusted accordingly. Due to the substantial CPU time required to perform this process to a high degree of precision, a large tolerance on the specified mixture ratio was allowed.

Simulations are initiated by partially filling the combustion chamber with a fuel and air premixture at ambient (atmospheric) conditions. The inlet valve is closed. The fuel and air mixture is then ignited with a small kernel of high temperature, high pressure air placed at the centerline, just downstream of the diverter aft face. The resulting small blast wave typically yields resonant operation within a few cycles.

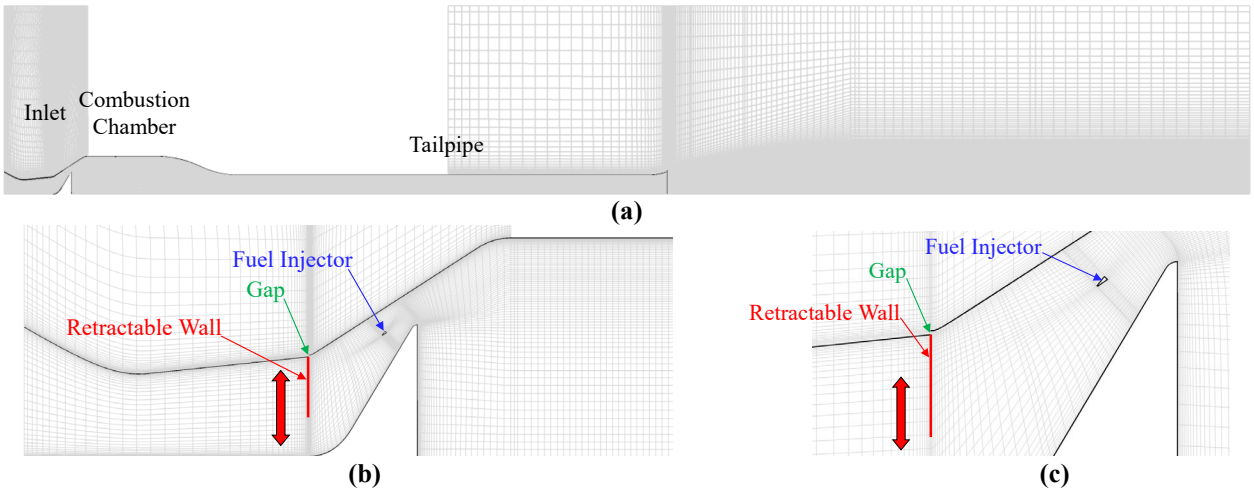

Fig. 5 Full computational domain (a); inlet detail (b); leakage gap detail (c). Approximately every other grid point is shown in both axial and radial directions. The tailpipe diameter is 1.25 in. The overall length is 22 in.

A. Dwell Period Optimization

The first, and main parameter considered in this work was τ_{dwell} (see Fig. 4). The duration of τ_{oc} was fixed at 0.5 msec., corresponding to a nominal disc rotational speed of 6,000 rpm. The value of τ_{dwell} was then selected. The value of τ_{closed} was determined by a notional feedback pressure sensor located on the centerline, just downstream of the diverter aft face. When the pressure here dropped below ambient, the valve cycle would restart, and the opening process would begin again. The simulation would repeat this process until a near limit cycle was achieved. All optimization simulations were done without a leakage gap present. The gap geometry was in place, but the actual opening was replaced with a solid wall. Leakage effects were investigated separately and on a limited basis.

A plot of fuel specific impulse, I_{sp} and equivalence ratio, ER as functions of τ_{dwell} is shown in Fig. 6. All points represent an average over 4 cycles obtained after a limit cycle had been reached. It is apparent that I_{sp} rises as τ_{dwell} is increased up to a value of 1.0 msec. It is approximately level after that until τ_{dwell} exceeds 1.2 msec.

The value of ER is above 1.0 for all simulations. The reason for this will be discussed in Section IIIB. The main reason for presenting ER in this figure was to show that it is reasonably consistent for τ_{dwell} >0.6, and therefore is not influencing the I_{sp} trend.

Also shown in Fig. 6 as dashed green and blue lines are the experimental I_{sp} and ER obtained with the original reed valve used with this combustor [5]. The simulated rotary valved system, though admittedly somewhat idealized, outperforms the experimental reed valved system except at the lowest τ_{dwell} values. Part of the reason for this performance disparity is the fact that the experiment is fueled with liquid gasoline using a very crude venturi-type carburation system. Poor droplet distribution, atomization, mixing, and reaction are inevitable. In fact, this is one of the reasons that the present work has changed to gaseous propane. Another contributor to the performance disparity is the observation that the fully opened reed valve does not present a lossless flow path to the working fluid as does the rotary valve. Of course, the simulation is also adiabatic, and has a leakage free valve. Nevertheless, the performance enhancement indicated by Fig. 6, representing a pressure gain of approximately 90%, is an encouraging result for the rotary valve concept.

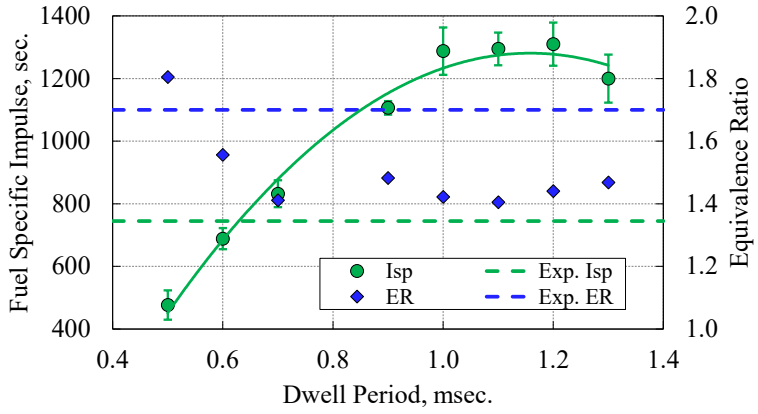

Fig. 6 Fuel specific impulse and equivalence ratio as functions of dwell period

The green bars in Fig. 6 represent the standard deviation in I_{sp} from the 4 cycles comprising each data point. When τ_{dwell} reaches 1.0 msec., it is seen that the standard deviation increases substantially. This is due to the development of a kind of dual pulse limit cycle behavior enabled by tying τ_{closed} to the chamber pressure. This means that the operating frequency is not fixed. With this arrangement, it is possible to obtain cyclic behavior illustrated by Fig. 7. Here I_{sp} and ER are shown for the 10th-15th cycle of the τ_{dwell} =1.0 msec. simulation. It is seen that the combustor has developed a persistent oscillation between two solutions. All measurable parameters cycle in this same manner (e.g. frequency, mass flow rate, etc.). The reason for this behavior is unknown as of this writing. It has been observed and noted in previous studies [17]. It is likely due to secondary acoustic waves or other periodic phenomena with fundamental modes that are well below that of the pulse combustor.

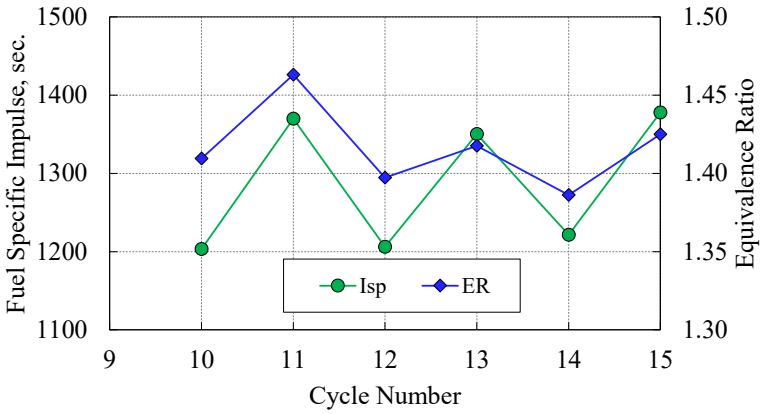

Fig. 7 Fuel specific impulse and equivalence ratio for the 10th-15th cycle of the τ_{dwell}=1.0 msec. simulation

Figure 8 shows cycle frequency and τ_{closed} as functions of τ_{dwell}. The data is averaged in the same manner as Fig. 6. The frequency dips then rises as τ_{dwell} rises, but the maximum deviation from the mean value of 235.3 Hz. is 0.7%. Meanwhile, the value of τ_{closed} drops significantly from 17% above the mean to 17% below. At peak performance levels, the ratio of τ_{closed} / (τ_{dwell}+2τ_{oc}) is approximately 1.0. For the reed valve testing of Ref. [13] this ratio was approximately 1.5. The standard deviation of frequency is also shown in Fig. 8. The variation in standard deviation with τ_{dwell} is similar to that of I_{sp} in Fig. 6.

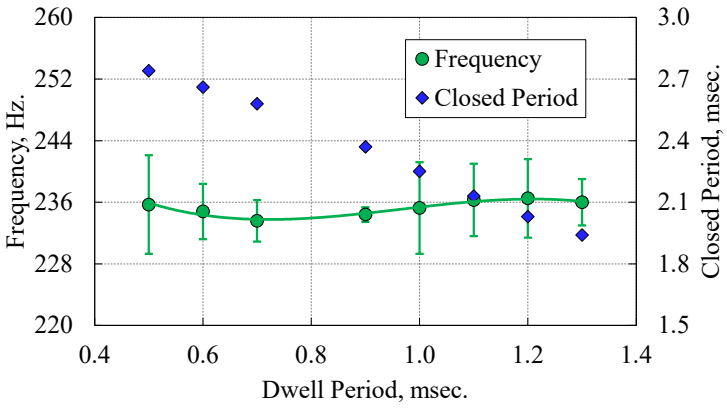

Fig. 8 Frequency and fully closed period as functions of dwell period

B. Equivalence Ratio Optimization

The impact of ER variation on both I_{sp} and thrust are shown in Fig. 9 for the τ_{dwell}=1.0 msec. simulation. An attempt to run the simulation at ER=1.0 resulted in a failed simulation. Though not shown here, trends similar to Fig. 9 were also observed with the τ_{dwell}=1.2 msec. simulation. A complete explanation for the observed trends is not clear as of this writing. Equivalence ratio changes certainly change chemical kinetics, which are likely to affect this highly coupled, multi-scale flow field. However, a more probable explanation involves where and when fuel is injected relative to the incoming air, and how it subsequently mixes. Stated another way, average or global ER is less important than local ER. By way of illustration, consider Fig. 10 which shows contours of temperature and fuel mass fraction in the combustion

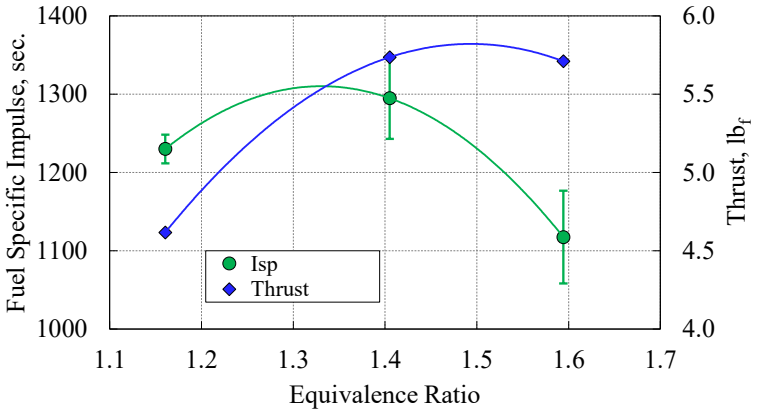

Fig. 9 Fuel specific impulse and thrust as functions of ER for the τ_{dwell}=1.1 msec. simulation

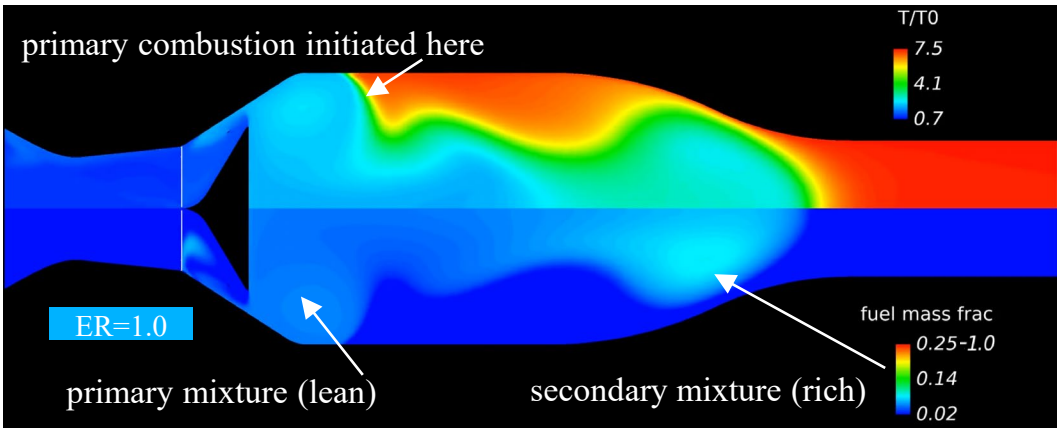

Fig. 10 Contours of temperature (upper half) and fuel mass fraction (lower half) in the combustion chamber of the τ_{dwell}=1.2 msec. simulation just as the valve is completing closure

chamber at a moment in time as the valve is completing closure. The color corresponding to *ER*=1.0 is shown in the lower left of the figure. At this point in time the rapid combustion has just started. A majority of the fluid that will react in the recirculating (vortex) region is labeled *primary mixture* in the figure. Note that this mixture is actually lean (ER<1.0). There is also a smaller *secondary mixture* that is rich; however, it is already leaving the combustion chamber and accelerating through the tailpipe. It will ultimately react, but the heat release will not contribute substantially to pressure gain. The existence of this secondary mixture is likely a combined result of the placement and sizing of the fuel injector ring, and injection at the wrong time. Injection time is difficult to control since it is based on a passive, pressure fed injection scheme. It might be influenced through the use of a tuned injection system, but this is beyond the scope of the present study. A cursory investigation of injector placement will be presented in the Section IIIC. Other influences on this secondary vortex formation likely include the combustor and diverter geometries. Previous studies [9, 17] have shown that alternative combustor geometries can result in improved fuel distribution and performance. However, combustor optimization is beyond the scope of the present study.

C. Injector Placement

The secondary mixture described above results from a secondary vortex that 'pinches off' from the primary starting vortex formed during the ingestion phase of the cycle. It can be seen at an earlier stage in Fig. 11 which is the same as Fig. 10 but at a different moment in time (ingestion). One possible way to mitigate the entrainment of fuel into this secondary region might be to change the radial location of the fuel injector. Figure 12 shows the outcome of such a conjecture. Here, I_{sp} and *ER* are shown for three different radial locations of the injector ring for the τ_{dwell} =1.1 msec.

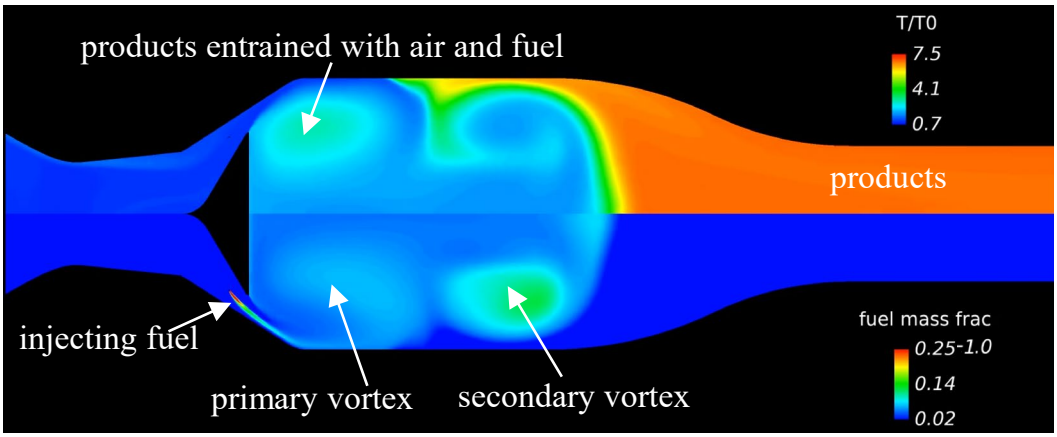

Fig. 11 Contours of temperature (upper half) and fuel mass fraction (lower half) in the combustion chamber of the τ_{dwell}=1.2 msec. simulation during ingestion when the valve is fully open

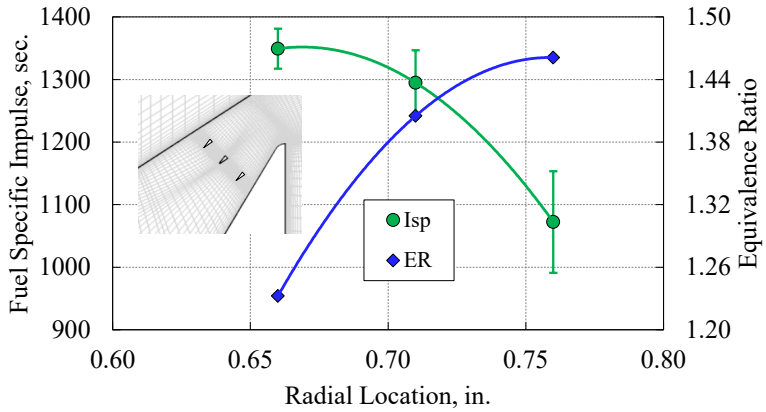

Fig.12 Fuel specific impulse and equivalence ratio for three radial injector positions for the τ_{dwell}=1.1 msec. simulation

case. The three injector locations are shown in the figure insert. The results indicate that as the fuel injector is moved radially inward (away from the fluid that will ultimately pinch off), performance improves.

There is considerably more optimization possible in terms of the injector location and orientation. However, these results give an early indicator for the planned experiment that injection holes placed on the diverter are preferred to having them at the location shown in Fig. 2.

D. Operation Without Valve Opening Feedback

The rotary disc valve system envisions a drive system where the duty cycle and rotational frequency are fixed. It is not expected to have the kind of feedback used up to this point (i.e., where opening commences when the chamber pressure drops below atmospheric). In order to examine this more realistic operation, three cases using τ_{dwell} = 1.0, 1.1, and 1.2 msec. were run to limit cycle operation with fixed τ_{closed} (i.e. fixed operational frequency). The operational frequency chosen was within a standard deviation of the 4 cycle averages shown in Fig. 8, but was not the exact average. The reason for this is that the simulations to be discussed were started before the feedback simulations had reached limit cycle operation. Running concurrent (as opposed to sequential) simulations was necessary due to scheduling constraints placed on completing the preliminary valve design. Results from the three fixed frequency simulations are shown in Fig. 13, which repeats Fig. 6 and adds the new points for comparison.

The τ_{dwell} = 1.0 and 1.2 msec. results are straightforward. The fixed frequency is within 0.6% of the mean frequency with feedback. The fixed *ER* and mean of feedback *ER* are close to one another, as are the two I_{sp} values. The τ_{dwell} = 1.0 msec. fixed ER is somewhat lower than the corresponding feedback ER; however, Fig. 9 indicates that relatively lean operation does not affect performance as strongly as relatively rich operation. Note that the fixed standard deviation in I_{sp} is significantly smaller than that of the feedback simulations since the dual pulse scenario described in Fig. 7 was absent.

The τ_{dwell} = 1.1 msec. results are the more perplexing. The fixed frequency is within 0.9% of the mean frequency with feedback. However, the fixed *ER* is significantly higher than the mean of feedback *ER* even though the fuel manifold pressures are identical. The reason that this occurs is still under investigation as of this writing, but the effect of its occurrence is consistent. Figure 9 showed a significant drop in I_{sp} as ER increases above 1.25 (i.e., rich operation). This makes sense since the extra fuel is likely not being utilized. As mixtures get extremely rich the combustion kinetics can be substantially affected which may lower thrust and further reduce I_{sp}. It appears as of now that τ_{dwell} = 1.1 msec. requires the two-solution behavior of Fig. 7 to achieve high performance, which is not practical for the envisioned rotary valve system.

In closing this section, it is worthwhile to note an anomalous result for the the τ_{dwell} = 1.0 msec. results. The results are not shown, but this simulation was initially run with a fixed frequency that was just 2.4% above the mean frequency with feedback. The result was an astonishing 50% drop in I_{sp} caused mostly by a 50% rise in *ER*. This result suggests that the rotary disc valve RPC performance is quite sensitive to fixed rotational speed; at least with the simple pressure fed fuel injection system used here.

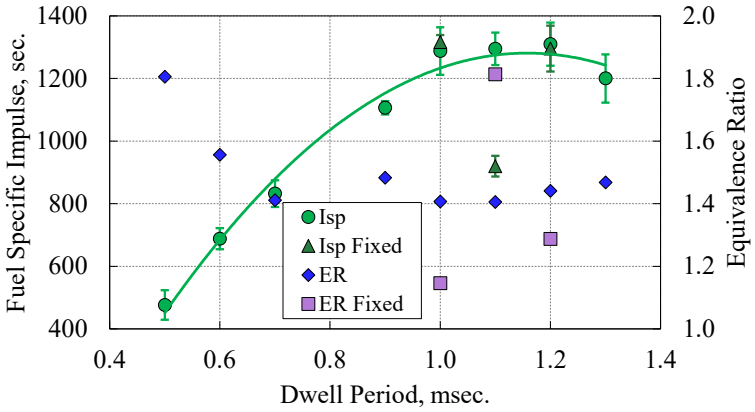

Fig.13 Fuel specific impulse and equivalence ratio for τ_{dwell}=1.0, 1.1, and 1.2 msec. at fixed τ_{dwell} (operational frequency)

E. Operation With Leakage

As a final exercise in assessing the rotary disc valve concept, the pulse combustor simulation was run to a limit cycle with the 0.01 in. leakage gap opened. A value of τ_{dwell} = 1.2 msec. was chosen, and operation was returned to the feedback based determination of τ_{closed}. This was done because it was expected that the optimal operating frequency would change with the addition of leakage. Ultimately however, the leakage gap had a very modest effect on performance. Table 1 compares various parameters of the τ_{dwell} = 1.2 msec. simulations with and without leakage. The fuel specific thrust dropped by approximately 11% with leakage. However, much of that drop is likely due to the lower *ER* where the leakage case settled. As discussed in Section IIIB (Fig. 9), operation at *ER*'s below approximately 1.3 results in lower performance. It is not clear why the leakage simulation resulted in lower *ER* than the original feedback case. The data indicates that the air flow rate increased while fuel flow rate stayed the same. It is correctable by raising the fuel manifold pressure. The leakage gap produces a net outflow of air that is approximately 5% of the inflow.

Contours of temperature (top half) and fuel mass fraction (bottom half) are shown for four different stages of the cycle with leakage in Fig. 14. Fluid is seen leaving the combustor through the gap, during the blowdown phase, and entering during the suction phase. There is a net flow out of the leakage gap amounting to approximately 5% of the main air flow.

It is noted that in the context of pressure gain combustion for gas turbines, this leakage flow could be usefully applied to cooling downstream turbomachinery blades. What leaks out is at the highest pressure in the cycle and it is almost entirely air (not combustion products). The issue of providing cooling flows in PGC systems is a recognized technology challenge, since they can no longer come from the compressor. Often, an auxiliary pump is envisioned. Capitalizing on the leakage flow observed here could substantially simplify the cooling challenge.

Table 1 Performance parameters for the simulations with τ_{dwell}=1.2 msec.

Case	Frequency Hz.	I_{sp} sec.	*ER*	Thrust lb_f
feedback	236.6	1309	1.44	5.74
fixed	238.1	1275	1.29	5.80
leakage	235.2	1190	1.14	5.06

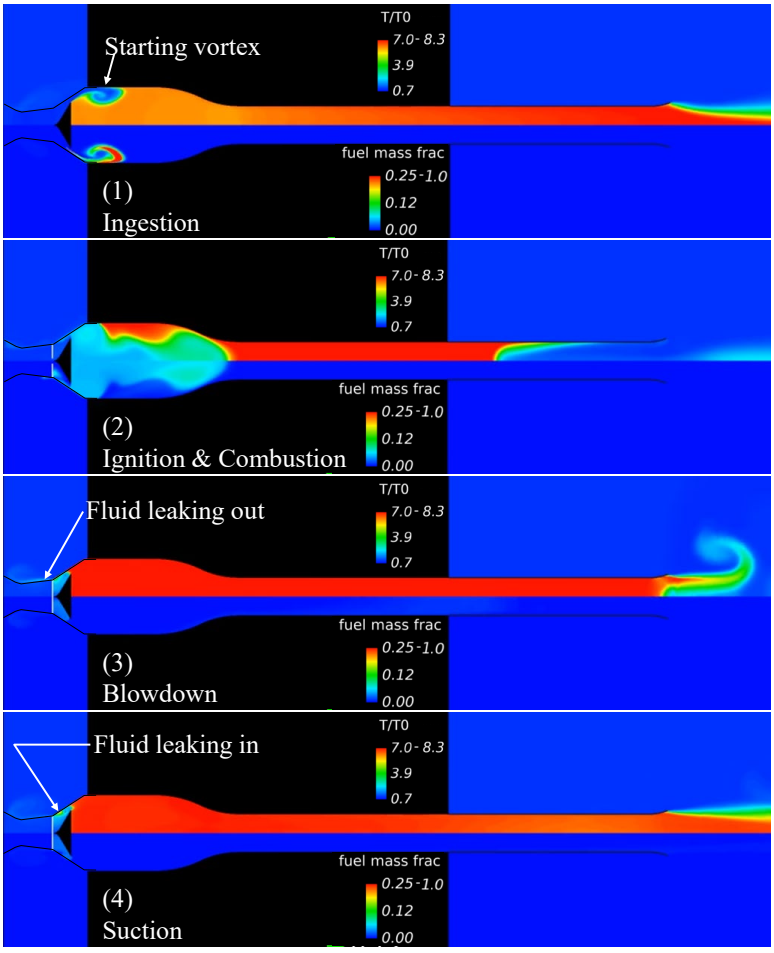

Fig.14 Simulated contours of temperature (upper half) and fuel mass fraction (lower half) from the τ_{dwell}=1.2 msec. configuration with leakage

IV. Preliminary Design

With the promising results detailed thus far, a preliminary experimental design was justified. A rendering of this design is shown in Fig. 15. The full assembly including combustion chamber and tailpipe is shown on the right. A detail of the rotary disc proper is shown on the left. The fuel injectors are not shown since their optimal placement is not yet established. As of this publication, no significant fabrication or potential operational issues (e.g. vibrations) have been identified.

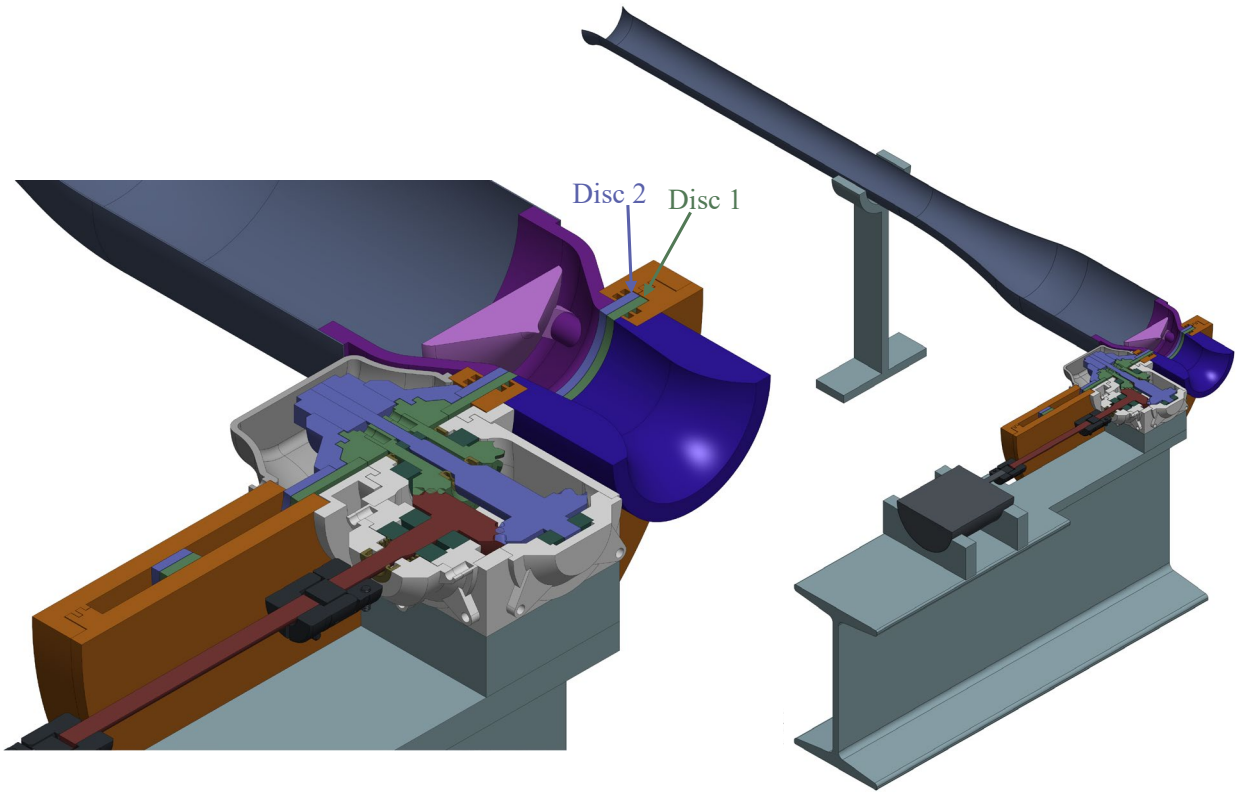

Fig. 15 Rendering of the rotary disc valve assembly design

V. Conclusion

A motor-driven, dual-disc, rotary air valve concept for a laboratory scale resonant pulse combustor (RPC) has been described. The concept is intended to simultaneously provide improved performance and extended valve life over the existing reed valves used on most RPC's. The valve motion has been optimized using a validated, axisymmetric, two-dimensional computational fluid dynamic simulation with a domain that includes the valve as a moveable interior wall. Variations in dwell period in the open position, closed period, fuel/air ratio, fuel injection location, and leakage have been examined in light of their effect on fuel specific impulse. Optimal configurations resulted in a fuel specific impulse improvement of more than 56% over that of the original reed valve. And areas where further improvements can be made, such as fuel injector placement, have been identified and discussed. Meanwhile, a preliminary mechanical design indicates that fabrication and operation of the concept valve present no significant challenges. These results further strengthen the case for RPC as a practical and promising implementation of pressure gain combustion for propulsion and power.

Acknowledgement

The authors would like to thank Shawn Dellinger of HX5 for his excellent mechanical design work on the subject rotary valve, and for providing Fig. 15. This work was supported by the NASA Transformational Tools and Technologies project under the Transformative Aeronautics Concepts Program.

Appendix A1

The chemical reaction mechanism consists of a single global propane reaction followed by a detailed (but reduced) model for the oxidation of CO and H2 as in the original Singh-Jachimowski mechanism [16]. Thus, the current and Singh-Jachimowski mechanisms differ only in the global fuel breakup reaction. The rate constants of the global propane reaction were selected to match ignition delay times obtained from a more detailed propane mechanism consisting of 41 species and 135 reactions. Figures A1.1 and A1.2 show comparisons of the two mechanisms. Note the good agreement in ignition delay times and equilibrium temperatures between the two mechanisms.

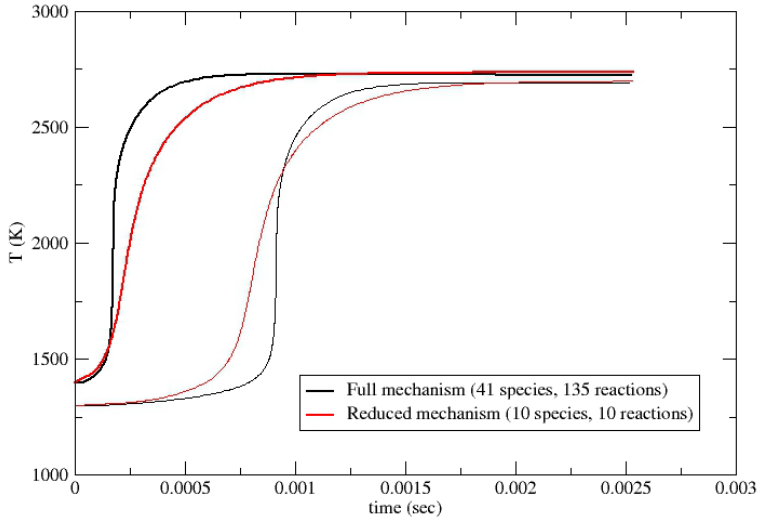

Fig. A1.1 Temperature as a function of time for the full and reduced propane mechanisms at two different initial temperatures. The pressure is 1.0 atmosphere. The equivalence ratio is 1.0.

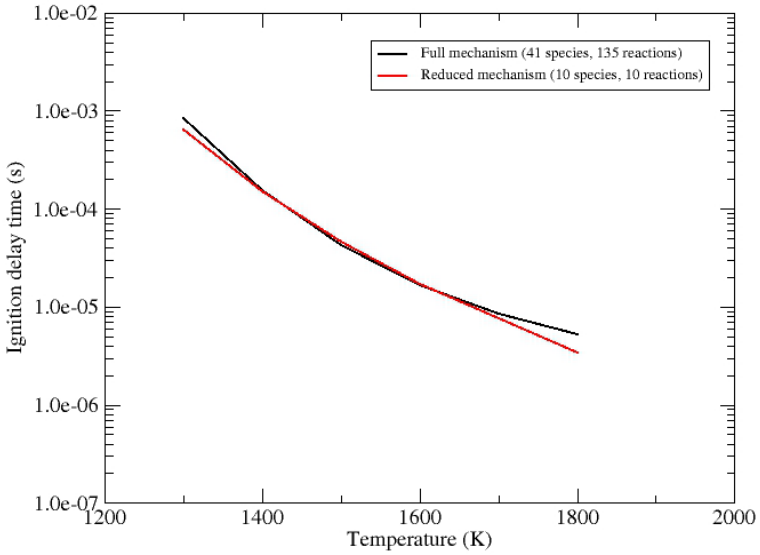

Fig. A1.2 Ignition delay time as a function of initial temperature for the full and reduced propane mechanisms. The pressure is 1.0 atmosphere. The equivalence ratio is 1.0.

References

[1] Brophy, C.M., Thoeny, A., "Geometry Impact on the Operation and Delivered Pressure Gain Characteristics of a Rotating Detonation Combustor," AIAA Paper 2024-2609, January 2024.

[2] Bach, E., et al., "Kiel Probes for Stagnation Pressure Measurement in Rotating Detonation Combustors," *AIAA Journal*, Vol. 60, No. 6, 2022, pp. 3724, 3735.

[3] Snyder, P.H., et al., "Pressure Gain Combustor Component Viability Assessment Based on Initial Testing," AIAA Paper 2011-5749, July 2011.

[4] Paxson, D.E., "Pressure-Gain Combustion for Gas Turbines," presented at the 2018 ASME Turbo Expo, Lillestrom, Norway, NASA TN55268, June 2018.

[5] Paxson, D.E., Wilson, J., and Dougherty, K., "Unsteady Ejector Performance: An Experimental Investigation Using a Pulsejet Driver," AIAA 2002-3915, July 2002.

[6] Kaemming, T.A., Paxson, D.E., "Determining the Pressure Gain of Pressure Gain Combustion," AIAA-2018-4567, July 2018.

[7] Paxson, D.E. and Dougherty, K., "Ejector Enhanced Pulsejet Based Pressure Gain Combustors: An Old Idea With a New Twist," AIAA 2005-4216, July 2005.

[8] Paxson, D.E., Dougherty, K.T., "Operability of an Ejector Enhanced Pulse Combustor in a Gas Turbine Environment," AIAA 2008-119, January 2008.

[9] Yungster, S., Paxson, D. E., Perkins, H. D., "Numerical Investigation of Shrouded Ejector-Enhanced Pulse Combustor Performance at High Pressure," *AIAA Journal of Propulsion and Power*, Vol. 33, No. 1, 2017, pp. 29-42.

[10] Kentfield, J.A.C, *Nonsteady, One-Dimensional, Internal, Compressible Flows*, Oxford University Press, 1993, p. 193.

[11] Yungster, S., Paxson, D. E., Perkins, H. D., "Computational Study of Pulsejet-Driven Pressure Gain Combustors at High-Pressure," AIAA 2013-3709, July 2013.

[12] Geng, T., Zheng, F., Kuznetsov, A.V., Roberts, W.L., Paxson, D.E., et al, "Comparison Between Numerically Simulated and Experimentally Measured Flowfield Quantities Behind a Pulsejet, Flow," *Turbulence and Combustion*, Vol. 84, No. 4, pp. 653-667, May 2010.

[13] Paxson, D.E., Yungster, S., Perkins, H. D., " Experimental and Computational Investigation of Valve Motion in a Resonant Pulse Combustor," AIAA-2024-1035, January 2024.

[14] Lisanti, J. C., Zhu, X., Guiberti, T. F., Roberts, W. L., "Active Valve Resonant Pulse Combustor for Pressure Gain Combustion Applications," *AIAA Journal of Propulsion and Power*, Vol. 38, No. 2, 2022, pp. 171-180.

[15] Yungster, S., Paxson, D. E., Perkins, H. D., "Computational Study of Pulsejet-Driven Pressure Gain Combustors at High-Pressure," AIAA 2013-3709, July 2013.

[16] Singh, D. J., Jachimowski, C. J., "Quasiglobal Reaction Model for Ethylene Combustion," *AIAA Journal*, Vol. 32, No 1, 1994, pp. 213-216.

[17] Yungster, S., Paxson, D. E., Perkins, H. D., "Computational Study of Compact Ejector-Enhanced Resonant Pulse Combustors," AIAA 2018-4786, July 2018.